EUROPEAN JOURNAL OF PURE AND APPLIED MATHEMATICS
2026, Vol. 19, Issue 3, Article Number 7841
ISSN 1307-5543 – ejpam.com
Published by New York Business Global

A Collocation Mittag-Leffler functions Approach for the Caputo Fractional Optimal Control Problems

Faizah A. H. Alomari

[1] *Department of Mathematics, Faculty of Science, Al-Baha University, Al-Baha, 65779, Saudi Arabia*

Abstract. In this study, a numerical approach based on Mittag-Leffler functions and collocation methods is proposed to solve multi-dimensional optimal control problems (MFOCPs) with mixed inequality constraints. First, we obtain the Mittag-Leffler operational matrix for fractional derivatives, which reduces the problem to a system of algebraic equations. Three examples were solved using this method to investigate its efficiency and accuracy. Detailed discussion of convergence properties and numerical results of the implemented method is provided for all three examples, which indicates that the proposed method has an exponential convergence. Our technique naturally handles inequality constraints through slack variables and Lagrange multipliers.

2020 Mathematics Subject Classifications: 49M05, 65T60, 26A33
Key Words and Phrases: Mittag-Leffler functions, collocation method, fractional optimal control, caputo derivative, inequality constraints.

1. Introduction

Optimal control theory is a significant mathematical tool in the areas of modern engineering and computational sciences, where it can be employed to optimize decision-making in dynamical systems. Since its early development in the 1950s by Pontryagin and Bellman, optimal control theory has been applied across almost all branches of science and engineering, ranging from aerospace navigation and robotic manipulation to economic systems and biomedicine. The traditional definition of OCPs employs integer-order differential equations, which satisfactorily model physical processes in which the rate of change is entirley dependent on the present state of the system. Nevertheless, numerous real-world systems involve memory and inheritance aspects that cannot be modeled using integer-order equations.

The use of fractional-order dynamic systems has gained considerable attention over the past two decades due to their ability to model physical phenomena exhibiting memory and hereditary characteristics [1–4]. The Fractional calculus is an extension of the conventional notions of differentiation and integration in terms of non-integer order, and thus

DOI: https://doi.org/10.29020/nybg.ejpam.v19i3.7841

Email address: faali@bu.edu.sa (Faizah A. H. Alomari)

 Copyright: © 2026 The Author(s). (CC BY-NC 4.0)

acts as a very powerful mathematical approach for the analysis of anomalous diffusion, viscoelasticity, electromagnetic waves, biological models, and financial systems, among others. Because the fractional derivative has the advantage of incorporating the whole history of a function in the expression, as opposed to classical integer-order derivatives, FOCPs emerge in several fields.

There are some difficulties that exist when formulating the mathematical theory associated with the FOCP, in comparison to when dealing with derivatives of integer order. The non-local nature of fractional derivatives makes it hard to formulate any optimality condition, especially since the fractional adjoint systems obtained may not have analytical solutions. Additionally, the existence of inequality constraints is another aspect that adds more difficulty to the process of formulation.

Numerical techniques that solve FOCP have been well-developed. These techniques can be distinguished into either indirect or direct techniques according to their way of solving such problems. Indirect techniques use the method of Pontryagin's maximum principle which translates an optimal control problem into a two-point boundary value problem using adjoint variables. In this way, indirect methods become very efficient in theory; however, there are some restrictions to their application due to the necessity of calculating optimality conditions and dependence on initial adjoint variables.

Direct methods discretize the state and control variables, thus transforming the optimal control problem from infinite dimension to finite dimension by changing the problem into a nonlinear programming problem (NLP). Direct methods are gaining popularity because of their robustness and easy implementation nature. In terms of effectiveness among all other direct methods, spectral accurate methods such as pseudospectral and collocation methods have gained popularity.

Recent literature has provided new insights to this subject. For instance, [5] offers an excellent review of spectral methods for solving FDE. On the other hand, [6] provides highly efficient operational matrix approaches. Finally, [7] presents recent developments related to high-performance computing when dealing with collocation methods to solve fractional differential equations. Other important contributions to this field include novel spectral methods for solving fractional differential equations [8], new operational matrix techniques for fractional systems [9], rigorous convergence analyses of collocation methods [10], and efficient numerical techniques for solving fractional optimal control problems [11].

Chebyshev polynomials provide good properties of interpolation, and therefore, they have been extensively applied for solving FOCPs since the application of the Chebyshev-Gauss-Lobatto points eliminates the problem of the Runge phenomenon, giving rise to exponential convergence in smooth functions [12, 13]. In addition, Bernoulli functions have been employed due to their operational matrices and straightforward application, whereas the piecewise property allows an adaptive solution of localized problems [14]. The block-pulse function system offers an easy way to transform fractional differential equations into algebraic equations using operational matrices. Hence, block-pulse functions are ideal candidates for solving differential equations with discontinuous control functions [15]. The Legendre polynomial is an essential tool in spectral methods due to its excellent convergence characteristics in L^2 space. Additionally, Legendre polynomials can

be related to Gaussian quadrature techniques [16, 17]. The Haar wavelet system possesses an important characteristic: multiresolution analysis [18, 19]. The Hermite polynomial is ideal for problems on an infinite domain or with weight functions in Gaussian form [20]. Pell-Lucas polynomials are among the recent additions to the list of orthogonal polynomials applicable to FOCPs, providing good results [21]. Lastly, the Legendre wavelet has the strengths of both wavelets (multi-resolution) and the spectral properties of Legendre polynomials [22]. Mehra et al. [23] presented a Legendre wavelet collocation scheme for FOCPs with a fractional Bolza objective function. Heydari et al. [1] investigated the variable-order fractional optimal control problem (VOFOCP), another difficult category of FOCPs in which the order of fractional derivatives depends on time.

Although significant progress has been made in optimal control problems, limited research has addressed inequality constraints in fractional optimal control theory, particularly in the context of Mittag-Leffler-type functions. Mittag-Leffler-type functions are recognized as natural solutions to fractional differential equations, and their formulation is presented as following:

$$E_{\xi,\eta}(z) = \sum_{k=0}^{\infty} \frac{z^k}{\Gamma(\xi k + \eta)}. \tag{1}$$

In integer-order systems, the exponential function e^z is the basic solution for differential equations. Thus, the natural connection of these functions to fractional calculus makes them suitable choices for constructing the bases of fractional problems. Several advantages motivate the use of Mittag-Leffler polynomials as basis functions:

(i) Natural representation: Solutions of fractional differential equations are often expressed in terms of Mittag-Leffler functions, leading to sparse representations when these functions are used as a basis.

(ii) Fractional calculus properties: The fractional derivative of a Mittag-Leffler function yields another Mittag-Leffler function, leading to simple operational matrices.

(iii) Spectral accuracy: Like other spectral methods, the Mittag-Leffler basis provides exponential convergence for smooth problems.

(iv) Parameter flexibility: The parameters ξ and η can be tuned to match the specific fractional order of the problem, potentially improving accuracy.

The presence of inequality constraints introduces significant challenges in fractional optimal control problems, which are:

(i) Inequality constraints lead to active/inactive sets that must be determined, requiring the solution of a constrained optimization problem rather than a system of equations.

(ii) The optimal control may exhibit nonsmooth behavior (e.g., bang-bang control) where the control switches between bounds, challenging spectral methods that assume smoothness.

Because of these problems, we use the slack variable method, which converts inequalities into equalities, enabling us to apply Lagrangian multipliers. The advantage of using the slack variable method is that it does not require previous knowledge of the active set.

2. Problem formulation

Consider the following general MFOCP:

$$\min J[X,V] = \int_0^1 \mathcal{L}\big(t, X(t), V(t)\big)\, dt, \tag{2}$$

subject to the fractional dynamical system:

$${}^{\mathrm{C}}\mathcal{D}_t^{\xi} X(t) = \Phi(t, X(t), V(t)), \quad 0 < \xi \leq 1, \tag{3}$$

inequality constraints

$$\mathcal{S}_j(t, X(t), V(t)) \leq 0, \quad j = 1, \ldots, m, \tag{4}$$

and the initial conditions

$$X(0) = X_0, \tag{5}$$

with ${}^{\mathrm{C}}\mathcal{D}_t^{\xi}$ stands for the Caputo fractional derivative operator, where $X(t) \in \mathbb{R}^n$ refers to the state variable, and $V(t) \in \mathbb{R}^p$ is the control variable, whereas $\mathcal{L}, \Phi, \mathcal{S}_j$ are continuously differentiable.

2.1. Notation

The following notation is considered consistently throughout this manuscript:

${}^{\mathrm{C}}\mathcal{D}_t^{\xi}$	Caputo fractional derivative of order ξ.
${}^{\mathrm{RL}}\mathcal{I}^{\xi}$	Riemann-Liouville fractional integral of order ξ.
$\Gamma(\cdot)$	Gamma function.
$\mathcal{E}_i^{\xi,\eta}(t)$	Mittag-Leffler polynomial of degree i.
$\mathbf{\Psi}_{\nu}^{\xi,\eta}(t)$	Vector of basis functions $[\mathcal{E}_0^{\xi,\eta}(t), \ldots, \mathcal{E}_{\nu}^{\xi,\eta}(t)]^{\mathsf{T}}$.
$\mathbf{C}, \mathbf{U}, \mathbf{S}, \mathbf{D}_{\xi}$	Vectors and matrices.
$L^2[0,1]$	Space of square-integrable functions on $[0,1]$.
$\|\cdot\|_2$, $\|\cdot\|_{L^2}$	Euclidean norm and L^2 norm.
$\otimes$	Kronecker product.
$(\cdot)^{\mathsf{T}}$	Transpose operator.

The paper is structured as follows. Section 3 recalls essential definitions from fractional calculus and introduces the Mittag-Leffler function. Section 4 discusses function approximation in the Mittag-Leffler basis. Section 5 derives the operational matrix for fractional differentiation. Section 6 presents the collocation methodology. Section 7 provides a convergence analysis. Finally, Section 8 presents numerical results for three examples.

3. Preliminaries

3.1. Fractional calculus

Definition 1. *For a function $w \in C^n[0,1]$ with $n-1 < \xi < n$, the Caputo fractional derivative is defined as*

$$ {}^{\mathrm{C}}\mathcal{D}_t^{\xi} w(t) = \frac{1}{\Gamma(n-\xi)} \int_0^t \frac{w^{(n)}(y)}{(t-y)^{\xi+1-n}}\, dy. \tag{6} $$

Definition 2. *The Riemann-Liouville fractional integral of order $\xi > 0$ is*

$$ {}^{\mathrm{RL}}\mathcal{I}^{\xi} w(t) = \frac{1}{\Gamma(\xi)} \int_0^t (t-y)^{\xi-1} w(y)\, dy. \tag{7} $$

The following properties will be employed throughout

$$ {}^{\mathrm{C}}\mathcal{D}_t^{\xi} t^{\beta} = \begin{cases} \dfrac{\Gamma(\beta+1)}{\Gamma(\beta+1-\xi)}\, t^{\beta-\xi}, & \beta > \lceil \xi \rceil - 1, \\ 0, & \beta \leq \lceil \xi \rceil - 1, \end{cases} \tag{8} $$

$$ {}^{\mathrm{RL}}\mathcal{I}^{\xi} \left({}^{\mathrm{C}}\mathcal{D}^{\xi} w(t) \right) = w(t) - \sum_{k=0}^{n-1} w^{(k)}(0^+) \frac{t^k}{k!}. \tag{9} $$

3.2. Mittag-Leffler functions

Definition 3. *For parameters $\xi > 0$, $\eta > 0$, and integer $i \geq 0$, the Mittag-Leffler functions are defined by*

$$ \mathcal{E}_i^{\xi,\eta}(t) = \sum_{k=0}^{i} \frac{t^{k\xi}}{\Gamma(\xi k + \eta)}, \quad t \in \mathbb{R}. \tag{10} $$

Lemma 1. *The set $\{\mathcal{E}_i^{\xi,\eta}(t)\}_{i=0}^{\infty}$ is complete in $L^2[0,1]$.*

Proof. The transformation $\mathbf{S}$ maps this basis to the monomial basis $\{t^{k\xi}\}_{k=0}^{\infty}$. The monomial basis with fractional powers is complete when $\xi > 0$ since the map $t \mapsto t^{\xi}$ is a homeomorphism of $[0,1]$. A rigorous proof follows from the Müntz–Szász theorem, which states that $\{t^{\lambda_k}\}$ is complete in $L^2[0,1]$ if $\sum 1/\lambda_k = \infty$; here $\lambda_k = k\xi$ satisfies this condition. See [24] for details.

These functions form a complete basis for $L^2[0,1]$ and possess convenient properties for fractional calculus applications. For $\xi = 1$, $\eta = 1$, we obtain the standard exponential polynomials.

4. Function approximation in the Mittag-Leffler functions basis

Let $\mathbb{L}^2 = L^2[0,1]$ denote the Hilbert space of square-integrable functions. Define the finite-dimensional subspace

$$\mathcal{Y}_\nu^{\xi,\eta} = \operatorname{span}\left\{\mathcal{E}_0^{\xi,\eta}, \mathcal{E}_1^{\xi,\eta}, \dots, \mathcal{E}_\nu^{\xi,\eta}\right\}. \tag{11}$$

- Define the standard L^2 inner product:

$$\langle f, g\rangle_{L^2} = \int_0^1 f(t)g(t)\,dt.$$

- Define the Gram matrix $\mathbf{G} \in \mathbb{R}^{(\nu+1)\times(\nu+1)}$ with entries:

$$\mathbf{G}_{ij} = \langle \mathcal{E}_i^{\xi,\eta}, \mathcal{E}_j^{\xi,\eta}\rangle_{L^2} = \int_0^1 \mathcal{E}_i^{\xi,\eta}(t)\mathcal{E}_j^{\xi,\eta}(t)\,dt.$$

- The orthogonal projection $P_\nu : L^2[0,1] \to \mathcal{Y}_\nu^{\xi,\eta}$ is then

$$P_\nu h = \Psi_\nu^{\xi,\eta}(t)^\top \mathbf{G}^{-1}\langle h, \Psi_\nu^{\xi,\eta}\rangle,$$

  where $\langle h, \Psi_\nu^{\xi,\eta}\rangle$ is the vector of inner products $[\langle h, \mathcal{E}_0^{\xi,\eta}\rangle, \dots, \langle h, \mathcal{E}_\nu^{\xi,\eta}\rangle]^\top$.

For any $h \in \mathbb{L}^2$, the orthogonal projection onto $\mathcal{Y}_\nu^{\xi,\eta}$ yields the best approximation

$$h(t) \approx h_\nu(t) = \sum_{i=0}^{\nu} c_i \mathcal{E}_i^{\xi,\eta}(t) = \mathbf{c}\mathbf{\Psi}_\nu^{\xi,\eta}(t), \tag{12}$$

where $\mathbf{\Psi}_\nu^{\xi,\eta}(t) = [\mathcal{E}_0^{\xi,\eta}(t), \dots, \mathcal{E}_\nu^{\xi,\eta}(t)]^\mathsf{T}$ and $\mathbf{c} = [c_0, \dots, c_\nu]$.

4.1. Transformation to monomial basis

The relationship between Mittag-Leffler function and monomial fractional bases is given by

$$\mathbf{\Psi}_\nu^{\xi,\eta}(t) = \mathbf{S}\mathbf{X}(t), \tag{13}$$

where $\mathbf{X}(t) = [1, t^\xi, t^{2\xi}, \dots, t^{\nu\xi}]^\mathsf{T}$ and $\mathbf{S}$ is the lower triangular matrix with entries:

$$\mathbf{S} = \begin{bmatrix} \frac{1}{\Gamma(\eta)} & 0 & 0 & \cdots & 0 \\ \frac{1}{\Gamma(\eta)} & \frac{1}{\Gamma(\xi+\eta)} & 0 & \cdots & 0 \\ \frac{1}{\Gamma(\eta)} & \frac{1}{\Gamma(\xi+\eta)} & \frac{1}{\Gamma(2\xi+\eta)} & \cdots & 0 \\ \vdots & \vdots & \vdots & \ddots & \vdots \\ \frac{1}{\Gamma(\eta)} & \frac{1}{\Gamma(\xi+\eta)} & \frac{1}{\Gamma(2\xi+\eta)} & \cdots & \frac{1}{\Gamma(\nu\xi+\eta)} \end{bmatrix}. \tag{14}$$

The set $\mathbf{\Psi}_{\nu}^{\xi,\eta}$ is linearly independent because $\mathbf{S}$ is invertible.

5. Operational matrix for fractional differentiation

Theorem 1. *The fractional derivative of the Mittag-Leffler function basis satisfies:*

$$ {}^{\mathrm{C}}\mathcal{D}_t^{\xi}\mathbf{\Psi}_{\nu}^{\xi,\eta}(t) = \mathbf{D}_{\xi}\mathbf{\Psi}_{\nu}^{\xi,\eta}(t), \tag{15}$$

where $\mathbf{D}_{\xi} = \mathbf{S}\mathbf{\Omega}\mathbf{S}^{-1}$ *and* $\mathbf{\Omega}$ *is given by*

$$ \mathbf{\Omega} = \begin{bmatrix} 0 & 0 & 0 & \cdots & 0 \\ \Gamma(\xi+1) & 0 & 0 & \cdots & 0 \\ 0 & \frac{\Gamma(2\xi+1)}{\Gamma(\xi+1)} & 0 & \cdots & 0 \\ \vdots & \vdots & \ddots & \ddots & \vdots \\ 0 & 0 & \cdots & \frac{\Gamma(\nu\xi+1)}{\Gamma((\nu-1)\xi+1)} & 0 \end{bmatrix}. \tag{16}$$

Proof. The Mittag-Leffler basis relates to the monomial fractional basis

$$\mathbf{X}(t) = [1, t^{\xi}, \ldots, t^{\nu\xi}]^{\mathsf{T}},$$

via

$$\mathbf{\Psi}_{\nu}^{\xi,\eta}(t) = \mathbf{S}\mathbf{X}(t),$$

where $\mathbf{S}$ is lower triangular in Eq. (14). Applying the Caputo derivative and using

$$\mathbf{X}(t) = \mathbf{S}^{-1}\mathbf{\Psi}_{\nu}^{\xi,\eta}(t).$$

Since $\mathbf{S}$ is a constant matrix and the Caputo fractional derivative ${}^{\mathrm{C}}\mathcal{D}_t^{\xi}$ is a linear operator, we have

$${}^{\mathrm{C}}\mathcal{D}_t^{\xi}\left(\mathbf{S}\mathbf{X}(t)\right) = \mathbf{S}\left({}^{\mathrm{C}}\mathcal{D}_t^{\xi}\mathbf{X}(t)\right).$$

This property is used to move $\mathbf{S}$ outside the derivative. From Eq. (8), we have

$$\begin{aligned}
{}^{\mathrm{C}}\mathcal{D}_t^{\xi}\mathbf{X}(t) &= [{}^{\mathrm{C}}\mathcal{D}_t^{\xi}1, {}^{\mathrm{C}}\mathcal{D}_t^{\xi}t^{\xi}, {}^{\mathrm{C}}\mathcal{D}_t^{\xi}t^{2\xi}, \ldots, {}^{\mathrm{C}}\mathcal{D}_t^{\xi}t^{\nu\xi}]^{\mathsf{T}} \\
&= [0, \frac{\Gamma(\xi+1)}{\Gamma(\xi+1-\xi)}t^{\xi-\xi}, \frac{\Gamma(2\xi+1)}{\Gamma(2\xi+1-\xi)}t^{2\xi-\xi}, \ldots, \frac{\Gamma(\nu\xi+1)}{\Gamma(\nu\xi+1-\xi)}t^{\nu\xi-\xi}]^{\mathsf{T}} \\
&= [0, \Gamma(\xi+1), \frac{\Gamma(2\xi+1)}{\Gamma(\xi+1)}t^{\xi}, \ldots, \frac{\Gamma(\nu\xi+1)}{\Gamma(\xi(\nu-1)+1)}t^{\xi(\nu-1)}]^{\mathsf{T}} \\
&= \begin{bmatrix} 0 & 0 & 0 & \cdots & 0 \\ \Gamma(\xi+1) & 0 & 0 & \cdots & 0 \\ 0 & \frac{\Gamma(2\xi+1)}{\Gamma(\xi+1)} & 0 & \cdots & 0 \\ \vdots & \vdots & \ddots & \ddots & \vdots \\ 0 & 0 & \cdots & \frac{\Gamma(\nu\xi+1)}{\Gamma((\nu-1)\xi+1)} & 0 \end{bmatrix} \begin{bmatrix} 1 \\ t^{\xi} \\ t^{2\xi} \\ \vdots \\ t^{\nu\xi} \end{bmatrix} \\
&= \mathbf{\Omega}\mathbf{X}(t).
\end{aligned}$$

Then

$$ {}^{\mathrm{C}}\mathcal{D}_t^{\xi}\mathbf{\Psi}_{\nu}^{\xi,\eta}(t) = \mathbf{S\Omega X}(t) = \mathbf{S\Omega S}^{-1}\mathbf{\Psi}_{\nu}^{\xi,\eta}(t). \tag{17} $$

Defining $\mathbf{D}_{\xi} = \mathbf{S\Omega S}^{-1}$ completes the proof.

6. Collocation method for constrained FOCPs

6.1. Function expansions

Let $\Psi_{\nu}^{\xi,\eta}(t) = [\mathcal{E}_0^{\xi,\eta}(t), \ldots, \mathcal{E}_{\nu}^{\xi,\eta}(t)]^{\mathsf{T}}$ be the Mittag-Leffler function basis. We approximate each component of the state and control variables as follows

For $i = 1, \ldots, n$:

$$ X_i(t) \approx X_i^{\nu}(t) = \mathbf{C}_i \Psi_{\nu}^{\xi,\eta}(t), \qquad \mathbf{C}_i \in \mathbb{R}^{1\times(\nu+1)}, $$

for $j = 1, \ldots, p$:

$$ V_j(t) \approx V_j^{\nu}(t) = \mathbf{U}_j \Psi_{\nu}^{\xi,\eta}(t), \qquad \mathbf{U}_j \in \mathbb{R}^{1\times(\nu+1)}, $$

the unknown coefficient vectors C_i and U_j are present in the aforementioned expressions

$$ \mathbf{C}_i = \left[c_0^i, c_1^i, \ldots, c_{\nu}^i\right], i = 1, 2, \ldots, n, \tag{18} $$

$$ \mathbf{U}_j = \left[u_0^j, u_1^j, \ldots, u_{\nu}^j\right], j = 1, 2, \ldots, p. \tag{19} $$

We assemble the coefficient matrices:

$$ \mathbf{C} = \begin{bmatrix}\mathbf{C}_1 & \mathbf{C}_2 & \cdots & \mathbf{C}_n\end{bmatrix} \in \mathbb{R}^{1\times(\nu+1)n}, $$

$$ \mathbf{U} = \begin{bmatrix}\mathbf{U}_1 & \mathbf{U}_2 & \cdots & \mathbf{U}_p\end{bmatrix} \in \mathbb{R}^{1\times(\nu+1)p}. $$

The full state and control vectors are then reconstructed as

$$ \begin{aligned} X(t) &= \left[\mathbf{C}_1\Psi_{\nu}^{\xi,\eta}(t), \mathbf{C}_2\Psi_{\nu}^{\xi,\eta}(t), \ldots, \mathbf{C}_n\Psi_{\nu}^{\xi,\eta}(t)\right]^T \\ &= \begin{bmatrix} \Psi_{\nu}^{\xi,\eta}(t)^{\mathsf{T}} & 0 & \cdots & 0 \\ 0 & \Psi_{\nu}^{\xi,\eta}(t)^{\mathsf{T}} & \cdots & 0 \\ \vdots & \vdots & \ddots & \vdots \\ 0 & 0 & \cdots & \Psi_{\nu}^{\xi,\eta}(t)^{\mathsf{T}} \end{bmatrix} \begin{bmatrix} \mathbf{C}_1^T \\ \mathbf{C}_2^T \\ \vdots \\ \mathbf{C}_n^T \end{bmatrix} \\ &= (I_n \otimes \Psi_{\nu}^{\xi,\eta}(t)^{\mathsf{T}})\mathbf{C}^{\mathsf{T}}, \end{aligned} \tag{20} $$

and

$$ \begin{aligned} V(t) &= \left[\mathbf{U}_1\Psi_{\nu}^{\xi,\eta}(t), \mathbf{U}_2\Psi_{\nu}^{\xi,\eta}(t), \ldots, \mathbf{U}_p\Psi_{\nu}^{\xi,\eta}(t)\right]^T \\ &= (I_p \otimes \Psi_{\nu}^{\xi,\eta}(t)^{\mathsf{T}})\mathbf{U}^{\mathsf{T}}. \end{aligned} \tag{21} $$

6.2. Inequality constraint treatment via slack variables

In this section, we employ the standard slack variable method [25]. Inequality constraints $\mathcal{S}_j(t, X(t), V(t)) \leq 0$ are converted to equalities using slack variables $z_j(t)$:

$$\mathcal{S}_j(t, X(t), V(t)) + z_j^2(t) = 0, \quad j = 1, \ldots, m.$$

Each slack variable is expanded in the same basis:

$$z_j(t) = \mathbf{Z}_j \Psi_\nu^{\xi,\eta}(t), \qquad \mathbf{Z}_j \in \mathbb{R}^{1\times(\nu+1)}.$$

6.3. Fractional differentiation operational matrix

From Theorem 1, the Caputo derivative of the basis satisfies

$${}^{\mathrm{C}}\mathcal{D}_t^\xi \Psi_\nu^{\xi,\eta}(t) = \mathbf{D}_\xi \Psi_\nu^{\xi,\eta}(t),$$

where $\mathbf{D}_\xi = \mathbf{S}\boldsymbol{\Omega}\mathbf{S}^{-1}$. Thus, for the state vector

$${}^{\mathrm{C}}\mathcal{D}_t^\xi X(t) \approx (I_n \otimes \mathbf{D}_\xi \Psi_\nu^{\xi,\eta}(t)^{\mathsf{T}})\mathbf{C}^{\mathsf{T}}.$$

6.4. Collocation points

The choice of collocation points critically affects the accuracy and stability of the numerical method. Three types of collocation points are considered in this work, which are commonly used in spectral methods:

6.4.1. Chebyshev-Gauss-Lobatto (CGL) points

Chebyshev-Gauss-Lobatto points are the most widely used collocation points for spectral methods. They are defined as the extrema of the Chebyshev polynomial $T_\nu(x) = \cos(\nu \arccos x)$:

$$t_k = \frac{1}{2}\left(1 - \cos\frac{k\pi}{\nu}\right), \quad k = 0, 1, \ldots, \nu. \tag{22}$$

These points are optimal for polynomial interpolation because they minimize the Runge phenomenon and provide exponential convergence for smooth functions. The points are clustered near the boundaries, which helps control interpolation errors.

6.4.2. Legendre-Gauss-Lobatto (LGL) points

Legendre-Gauss-Lobatto points are the roots of $(1-x^2)P'_\nu(x)$, where $P_\nu(x)$ is the Legendre polynomial of degree ν. These points are optimal for L^2-based spectral methods and are commonly used in *hp*-finite element methods. The LGL points satisfy:

$$\int_{-1}^{1} f(x)\,dx \approx \sum_{k=0}^{\nu} w_k f(x_k), \tag{23}$$

with exact integration for polynomials up to degree $2\nu-1$. The nodes on $[0, 1]$ are obtained by transforming from $[-1, 1]$ via $t_k = (x_k + 1)/2$.

6.4.3. Uniform points

Uniform points are the equally spaced points:

$$t_k = \frac{k}{\nu}, \quad k = 0, 1, \ldots, \nu. \tag{24}$$

They are simple to implement; however, they suffer from the Runge phenomenon for high-degree polynomial interpolation and are generally not recommended for spectral methods.

6.5. Discretization of the system

At each collocation point t_k, we enforce:
Dynamical system: For $i = 1, \ldots, n$ and $k = 1, \ldots, \nu$:

$$(I_n \otimes \mathbf{D}_\xi \Psi_\nu^{\xi,\eta}((t_k))^\mathsf{T})\mathbf{C}^\mathsf{T} = \Phi\big(t_k,\ (I_n \otimes \Psi_\nu^{\xi,\eta}(t_k)^\mathsf{T})\mathbf{C}^\mathsf{T},\ (I_p \otimes \Psi_\nu^{\xi,\eta}(t_k)^\mathsf{T})\mathbf{U}^\mathsf{T}\big).$$

Inequality constraints: For $j = 1, \ldots, m$ and $k = 0, \ldots, \nu$:

$$\mathcal{S}_j\big(t_k,\ (I_n \otimes \Psi_\nu^{\xi,\eta}(t_k)^\mathsf{T})\mathbf{C}^\mathsf{T},\ (I_p \otimes \Psi_\nu^{\xi,\eta}(t_k)^\mathsf{T})\mathbf{U}^\mathsf{T}\big) + \big(\mathbf{Z}_j \Psi_\nu^{\xi,\eta}(t_k)\big)^2 = 0.$$

6.6. Augmented Lagrangian and optimality conditions

Define the augmented Lagrangian:

$$\mathcal{L}^* = J(\mathbf{C}, \mathbf{U}) + \sum_{k=0}^{\nu} \sum_{r=0}^{m} \lambda_{rk}\, \mathcal{H}_r(t_k),$$

where

- $\mathcal{H}_0(t_0) := (I_n \otimes \Psi_\nu^{\xi,\eta}(0)^\mathsf{T})\mathbf{C}^\mathsf{T} - X_0$,
- $\mathcal{H}_0(t_k) := (I_n \otimes \mathbf{D}_\xi \Psi_\nu^{\xi,\eta}((t_k))^\mathsf{T})\mathbf{C}^\mathsf{T} - \Phi\big(t_k,\ (I_n \otimes \Psi_\nu^{\xi,\eta}(t_k)^\mathsf{T})\mathbf{C}^\mathsf{T},\ (I_p \otimes \Psi_\nu^{\xi,\eta}(t_k)^\mathsf{T})\mathbf{U}^\mathsf{T}\big)$ (dynamical residual) for $k = 1, \ldots, \nu$, and
- $\mathcal{H}_r(t_k) := \mathcal{S}_r\big(t_k,\ (I_n \otimes \Psi_\nu^{\xi,\eta}(t_k)^\mathsf{T})\mathbf{C}^\mathsf{T},\ (I_p \otimes \Psi_\nu^{\xi,\eta}(t_k)^\mathsf{T})\mathbf{U}^\mathsf{T}\big) + \big(\mathbf{Z}_r \Psi_\nu^{\xi,\eta}(t_k)\big)^2$ for $r = 1, \ldots, m$ and for $k = 0, \ldots, \nu$ (inequality residual).

The necessary optimality conditions are

$$\frac{\partial \mathcal{L}^*}{\partial \mathbf{C}_i} = 0\ \ (i = 1, \ldots, n), \quad \frac{\partial \mathcal{L}^*}{\partial \mathbf{U}_j} = 0\ \ (j = 1, \ldots, p), \quad \frac{\partial \mathcal{L}^*}{\partial \mathbf{Z}_j} = 0\ \ (j = 1, \ldots, m), \quad \frac{\partial \mathcal{L}^*}{\partial \lambda_{rk}} = 0\ \ (\forall r, k). \tag{25}$$

These conditions form a system of nonlinear algebraic equations

$$\{\mathbf{C}_i\}_{i=1}^n,\ \{\mathbf{U}_j\}_{j=1}^p,\ \{\mathbf{Z}_j\}_{j=1}^m,\ \{\lambda_{rk}\}.$$

6.7. Newton's method

The algebraic system is solved using Newton's method. Let $\mathcal{Y}$ denote the vector of all unknowns. At each iteration:

(i) Compute the residual $F(\mathcal{Y})$.

(ii) Compute the Jacobian matrix $J_F = \partial F/\partial \mathcal{Y}$.

(iii) Solve $J_F\,\Delta\mathcal{Y} = -F$.

(iv) Update $\mathcal{Y} \leftarrow \mathcal{Y} + \Delta\mathcal{Y}$.

The process is repeated until $\|F(\mathcal{Y})\| < \text{tol}$.

6.8. Algorithm

Algorithm 1 Collocation Mittag-Leffler method for constrained FOCPs

Require: Fractional order ξ, parameter η, number of basis functions ν, collocation type (CGL/LGL/Uniform), system dimensions n, p, m.

Ensure: Approximate state $X(t) = (I_n \otimes \Psi_\nu^{\xi,\eta}(t)^{\mathsf{T}})\mathbf{C}^{\mathsf{T}}$ and control $V(t) = (I_p \otimes \Psi_\nu^{\xi,\eta}(t)^{\mathsf{T}})\mathbf{U}^{\mathsf{T}}$.

```
Generate collocation points {t_k}_{k=0}^{ν} according to chosen type.
Construct Mittag-Leffler basis Ψ_ν^{ξ,η}(t).
Form operational matrix D_ξ = SΩS^{-1}.
Initialize coefficient matrices C, U, Z and multipliers λ_rk.
for k = 0 to ν do
    for j = 0 to m do
        H_j(t_k) = 0
    end for
end for
Form augmented Lagrangian L* and derive optimality conditions.
Solve the resulting algebraic system (25) using Newton's method.
Return C, U.
```

7. Convergence analysis

Theorem 2. *Let $w \in C^{\nu+1}[0,1]$ and let w_ν be its best approximation in $\mathcal{Y}_\nu^{\xi,\eta}$. Then*

$$\|w - w_\nu\|_{L^2} \le \frac{\delta}{(\nu+1)!\sqrt{2\nu+3}}, \tag{26}$$

where $\delta = \max_{t\in[0,1]} |w^{(\nu+1)}(t)|$.

Proof. For any $w \in C^{\nu+1}[0,1]$, the Taylor expansion with integral remainder at $t = 0$ gives:

$$w(t) = \sum_{k=0}^{\nu} \frac{w^{(k)}(0)}{k!} t^k + R_\nu(t), \quad R_\nu(t) = \int_0^t \frac{(t-s)^\nu}{\nu!} w^{(\nu+1)}(s)\, ds. \tag{27}$$

The remainder satisfies

$$|R_\nu(t)| \leq \frac{\delta}{(\nu+1)!} t^{\nu+1} \leq \frac{\delta}{(\nu+1)!},$$

for $t \in [0,1]$. The polynomial:

$$p_\nu(t) = \sum_{k=0}^{\nu} \frac{w^{(k)}(0)}{k!} t^k,$$

belongs to the space of polynomials of degree ν in t. Since the Mittag-Leffler basis $\mathcal{Y}_\nu^{\xi,\eta}$ contains all such polynomials (via the invertible transformation $\mathbf{S}$), we have $p_\nu \in \mathcal{Y}_\nu^{\xi,\eta}$. By the optimality of w_ν as the best approximation in $\mathcal{Y}_\nu^{\xi,\eta}$,

$$\|w - w_\nu\|_{L^2} \leq \|w - p_\nu\|_{L^2} = \|R_\nu\|_{L^2} \leq \left(\int_0^1 \left(\frac{\delta}{(\nu+1)!} \right)^2 dt \right)^{1/2} = \frac{\delta}{(\nu+1)!}. \tag{28}$$

A sharper bound using the fact that

$$|R_\nu(t)| \leq \frac{\delta}{(\nu+1)!} t^{\nu+1},$$

yields

$$\|R_\nu\|_{L^2}^2 \leq \frac{\delta^2}{((\nu+1)!)^2} \int_0^1 t^{2\nu+2} dt = \frac{\delta^2}{((\nu+1)!)^2 (2\nu+3)},$$

completing the proof. □

Lemma 2 (Norm equivalence)**.** *The transformation* $\mathbf{S}$ *induces a norm equivalence between the coefficient space and the* L^2 *norm. Specifically, there exist constants* $0 < c_1 \leq c_2$ *such that for any* $\mathbf{c} \in \mathbb{R}^{\nu+1}$*,*

$$c_1 \|\mathbf{c}\|_{\ell^2} \leq \|\mathbf{c}^\mathsf{T} \mathbf{\Psi}_\nu^{\xi,\eta}\|_{L^2} \leq c_2 \|\mathbf{c}\|_{\ell^2}. \tag{29}$$

Moreover, the condition number $\kappa(\mathbf{S}) = \|\mathbf{S}\|_2 \|\mathbf{S}^{-1}\|_2$ *remains bounded independently of* ν *for fixed* ξ, η*.*

Theorem 3. *For analytic functions* w *on* $[0,1]$*, then*

$$\|w - w_\nu\|_{L^2} \longrightarrow 0. \tag{30}$$

Proof. The Mittag-Leffler basis $\mathbf{\Psi}_{\nu}^{\xi,\eta}$ is isomorphic to the monomial fractional basis $\{1, t^{\xi}, t^{2\xi}, \ldots, t^{\nu\xi}\}$ via the invertible transformation $\mathbf{S}$. Consequently, the approximation space $\mathcal{Y}_{\nu}^{\xi,\eta}$ is equivalent to the space of polynomials of degree ν in t^{ξ}.

To rigorously extend classical polynomial approximation theory to the fractional-power basis, we employ a change of variable. Define $s = t^{\xi}$, where $\xi > 0$. The map $t \mapsto s = t^{\xi}$ is a strictly increasing C^{∞} homeomorphism from $[0,1]$ onto $[0,1]$. Its inverse is $t = s^{1/\xi}$, which is also smooth on $(0,1]$ and continuous on $[0,1]$.

Now consider any analytic function $w(t)$ on $[0,1]$. Define the composition $\tilde{w}(s) = w(s^{1/\xi})$ for $s \in [0,1]$. Since w is analytic on $[0,1]$ and $s \mapsto s^{1/\xi}$ is analytic on $(0,1]$ with a removable singularity at $s = 0$ (as $\xi > 0$), the function $\tilde{w}(s)$ is also analytic on $[0,1]$. Therefore, $\tilde{w}$ admits an analytic extension to a complex ellipse E_{ρ} with foci at 0 and 1 and parameter $\rho > 1$.

Classical approximation theory (see, [26]) states that for analytic functions, the Chebyshev polynomial approximation error decays exponentially. Hence, there exists a polynomial $p_{\nu}(s)$ of degree ν in s such that:

$$\|\tilde{w} - p_{\nu}\|_{\infty} \leq C\rho^{-\nu}, \tag{31}$$

where $C > 0$ is a constant and $\rho > 1$ depends on the region of analyticity.

Transforming back via $t = s^{1/\xi}$, we obtain $p_{\nu}(t^{\xi})$, which lies in the span of $\{1, t^{\xi}, t^{2\xi}, \ldots, t^{\nu\xi}\}$. Since this fractional monomial space is isomorphic to $\mathcal{Y}_{\nu}^{\xi,\eta}$ via the invertible transformation $\mathbf{S}$, the function $p_{\nu}(t^{\xi})$ belongs to $\mathcal{Y}_{\nu}^{\xi,\eta}$.

The L^2 norm is bounded by the maximum norm on $[0,1]$, so:

$$\|w - p_{\nu}(t^{\xi})\|_{L^2} \leq \|w - p_{\nu}(t^{\xi})\|_{\infty} = \|\tilde{w} - p_{\nu}\|_{\infty} \leq C\rho^{-\nu}. \tag{32}$$

Since w_{ν} is the best L^2 approximation in $\mathcal{Y}_{\nu}^{\xi,\eta}$, we have:

$$\|w - w_{\nu}\|_{L^2} \leq \|w - p_{\nu}(t^{\xi})\|_{L^2} \leq C\rho^{-\nu}. \tag{33}$$

Thus, $\|w - w_{\nu}\|_{L^2} = \mathcal{O}(\rho^{-\nu})$, which is exponential convergence because $\rho^{-\nu} = e^{-\nu \ln \rho}$.

Theorem 4 (Conditioning)**.** *The condition number of the collocation matrix $\mathbf{\Psi}_{coll}$ with entries $\Psi_{ik} = \mathcal{E}_{k}^{\xi,\eta}(t_i)$ satisfies*

$$\kappa(\mathbf{\Psi}_{coll}) \leq \|\mathbf{S}\|_2 \|\mathbf{S}^{-1}\|_2 \kappa(\mathbf{X}_{coll}), \tag{34}$$

where $\mathbf{X}_{coll}$ is the monomial collocation matrix. For $\nu \leq 15$ and well-chosen collocation points (CGL or LGL), $\kappa(\mathbf{\Psi}_{coll}) < 10^6$ in double-precision arithmetic.

8. Numerical experiments

Example 1

Consider the linear quadratic fractional optimal control problem

$$\begin{aligned} \min J &= \frac{1}{2}\int_0^1 \left(X^2(t) + V^2(t)\right) dt, \\ \text{s.t.} \quad {}^{\mathrm{C}}\mathcal{D}_t^{\xi} X(t) &= -X(t) + V(t), \quad X(0) = 1. \end{aligned} \tag{35}$$

For $\xi = 1$, the exact solution is known and given by

$$X(t) = \cosh(\sqrt{2}t) + \beta \sinh(\sqrt{2}t),$$
$$V(t) = (1 + \sqrt{2}\beta)\cosh(\sqrt{2}t) + (\sqrt{2} + \beta)\sinh(\sqrt{2}t),$$

where $\beta = -\dfrac{\cosh(\sqrt{2}) + \sqrt{2}\sinh(\sqrt{2})}{\sqrt{2}\cosh(\sqrt{2}) + \sinh(\sqrt{2})}$. Three types of collocation points were tested with $\nu = 4$ (5 points), and the results are shown in figure 1. Table 1 presents the numerical results obtained with each collocation point type. In Table 2 and figure 2, we present a convergence study for example 1 with CGL points. In figure 3, we present the error in vs t for example 1. In figure 4, we comparison of state and control variables obtained with different collocation points for example 1. As one can see from the results shown in table 1, CGL points yield the smallest maximum state error (1.86×10^{-4}) and control error (5.65×10^{-4}).

- Chebyshev-Gauss-Lobatto (CGL): 0.0000, 0.1464, 0.5000, 0.8536, 1.0000.
- Legendre-Gauss-Lobatto (LGL): 0.0000, 0.5000, 0.5777, 0.9184, 1.0000.
- Uniform: 0.0000, 0.2500, 0.5000, 0.7500, 1.0000.

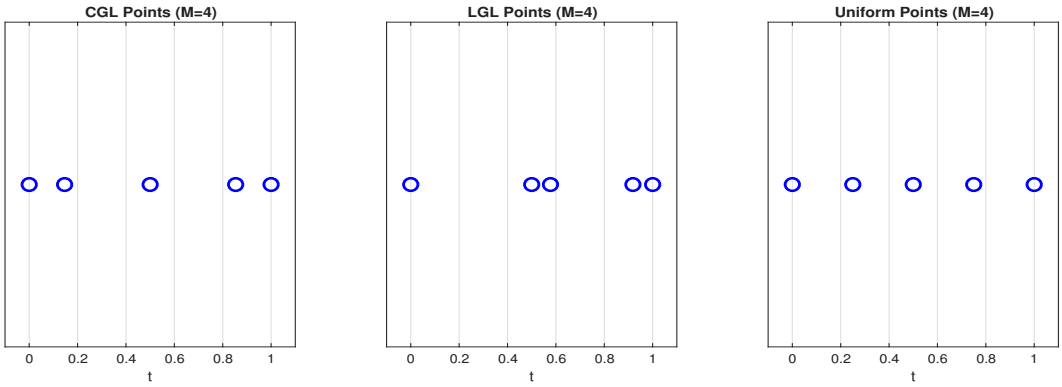

Figure 1: Three types of collocation points were tested with $\nu = 4$ (5 points).

Table 1: Numerical results for example 1 with $\xi = 1$, $\nu = 4$.

Points	J	$\max \lvert X - X_{\text{exact}} \rvert$	$\max \lvert V - V_{\text{exact}} \rvert$
CGL	0.19289180	1.86×10^{-4}	5.65×10^{-4}
LGL	0.19276792	8.13×10^{-4}	1.69×10^{-3}
Uniform	0.19288010	2.26×10^{-4}	6.56×10^{-4}

Table 2: Convergence study for example 1 with CGL points.

ν	L^2 error (state)	L^2 error (control)	Convergence rate
4	9.74×10^{-5}	3.53×10^{-4}	—
6	2.15×10^{-7}	1.41×10^{-6}	1.010
8	9.56×10^{-9}	8.27×10^{-8}	1.013
10	9.76×10^{-10}	1.01×10^{-8}	1.027

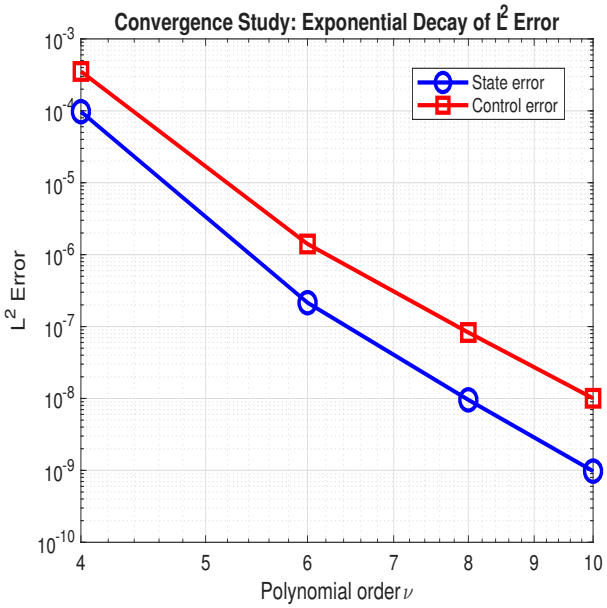

Figure 2: Convergence study for example 1.

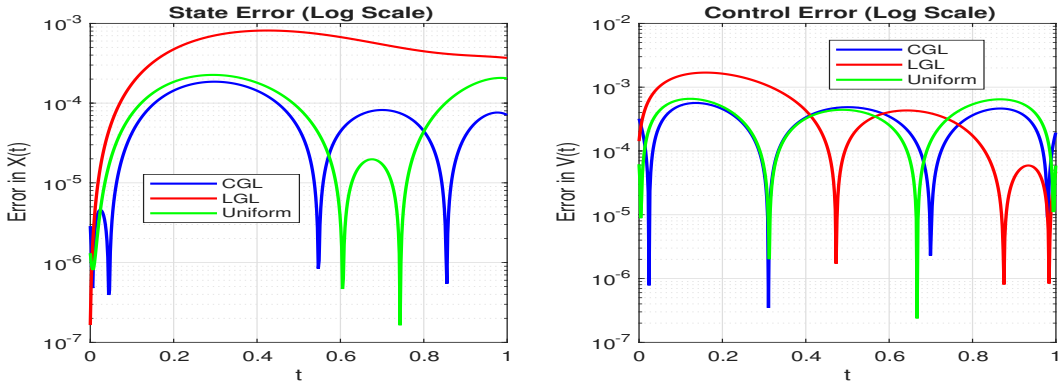

Figure 3: Error in vs t for example 1.

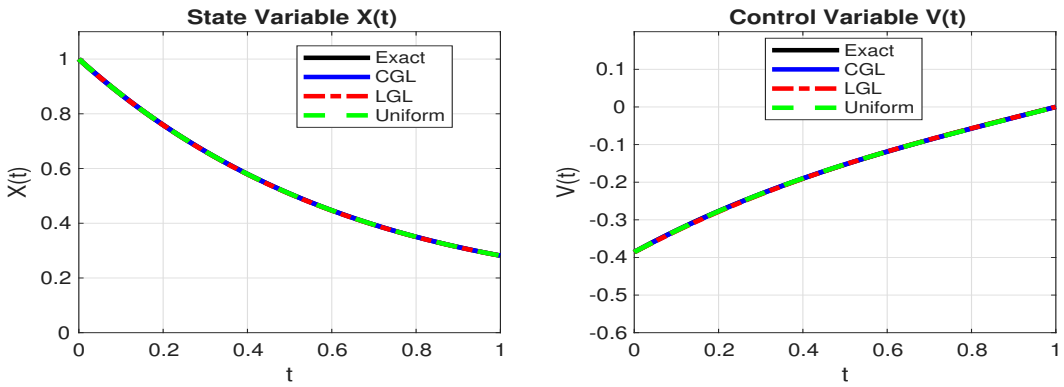

Figure 4: Comparison of state and control variables obtained with different collocation points for example 1.

Example 2

Consider the fractional optimal control problem with inequality constraints:

$$\begin{aligned} \min J &= \frac{1}{2}\int_0^1 \left(X_1^2(t) + V^2(t)\right) dt, \\ \text{s.t.} \quad {}^{\mathrm{C}}\mathcal{D}_t^{\xi} X_1(t) &= X_2(t), \\ {}^{\mathrm{C}}\mathcal{D}_t^{\xi} X_2(t) &= -X_2(t) + V(t), \\ |V(t)| &\le 1, \\ X_1(0) = 0, &\quad X_2(0) = 10. \end{aligned} \tag{36}$$

For $\xi = 1$, the exact optimal cost is known to be $J \approx 8.07054$ from the literature [25]. Three types of collocation points were tested with $\nu = 4$ (5 points):

- Chebyshev-Gauss-Lobatto (CGL): 0.0000, 0.1464, 0.5000, 0.8536, 1.0000.
- Legendre-Gauss-Lobatto (LGL): 0.0000, 0.5000, 0.5777, 0.9184, 1.0000.
- Uniform: 0.0000, 0.2500, 0.5000, 0.7500, 1.0000.

Table 3 presents the numerical results obtained with each collocation point type for $\nu = 4$, and Table 4 for $\nu = 9$. The solution X obtained with different collocation points are illustrated in figure 5 and the control trajectories obtained with different collocation points are illustrated in figures 6 and 7. Based on the obtained results shown in Tables 3 and 4, it can be noted that all three methods give very close results ($J \approx 8.07377$). The results in this example are somewhat similar to the example in this article [25].

Table 3: Numerical results for example 2 with $\xi = 1$, $\nu = 4$.

Points	J	$\max V$	$\min V$
CGL	8.088897	-0.1913	-0.9685
LGL	8.088794	-0.1910	-0.9719
Uniform	8.127503	-0.5999	-0.9904

Table 4: Numerical results for example 2 with $\xi = 1$, $\nu = 9$.

Points	J	$\max V$	$\min V$
CGL	8.067734	-0.4694	-1.0020
LGL	8.064717	-0.4503	-1.0031
Uniform	8.008771	-0.0744	-1.0045

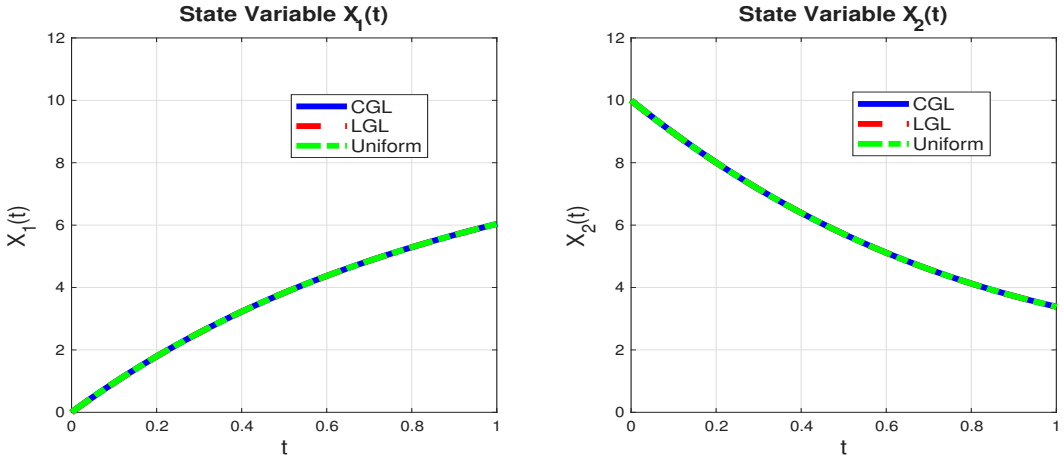

Figure 5: Comparison of $X(t)$ obtained with different collocation points for example 2.

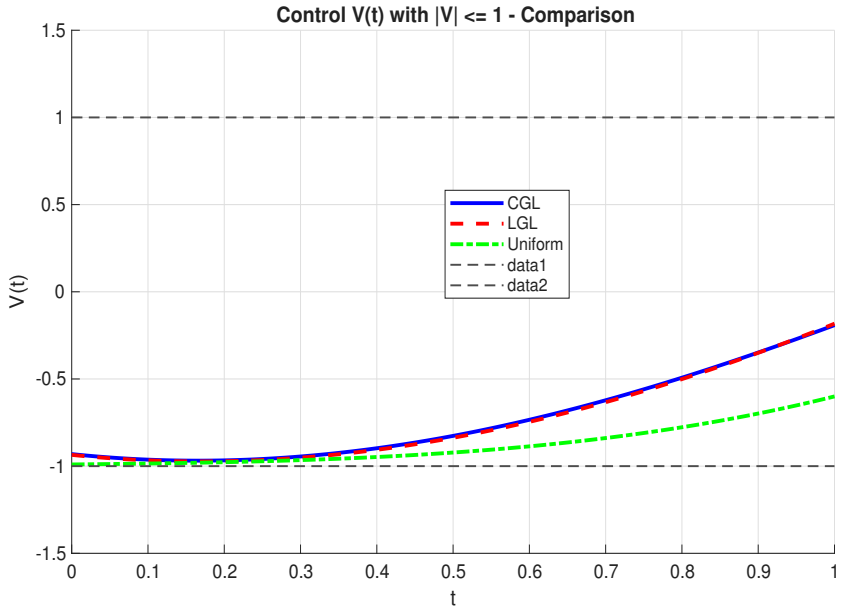

Figure 6: Comparison of control variable $V(t)$ obtained with different collocation points for example 2 for $\nu = 4$.

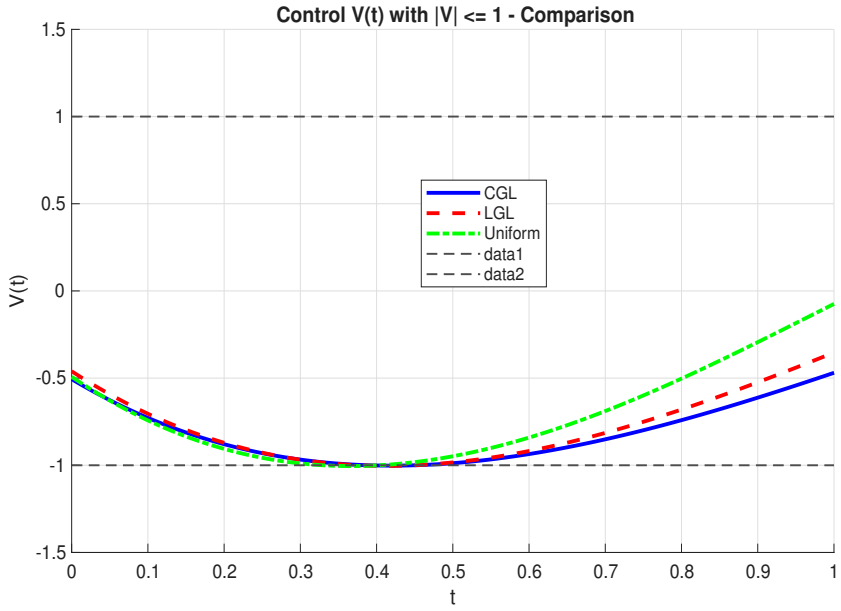

Figure 7: Comparison of control variable $V(t)$ obtained with different collocation points for example 2 for $\nu = 9$.

Example 3

Consider the following fractional optimal control problem designed to test exact solution recovery:

$$\begin{aligned} \min J &= \int_0^1 \left[(X(t) - t^\xi)^2 + (V(t) - t^\xi - \Gamma(\xi+1))^2 \right] dt, \\ \text{s.t.} \quad {}^{\mathrm{C}}\mathcal{D}_t^\xi X(t) &= -X(t) + V(t), \quad X(0) = 0. \end{aligned} \tag{37}$$

The exact solution is known to be:

$$X(t) = t^\xi, \qquad V(t) = t^\xi + \Gamma(\xi+1), \tag{38}$$

with optimal cost $J = 0$. For this test, we set $\xi = 0.5$ and $\nu = 2$ (3 collocation points). Three types of collocation points were tested with $\nu = 2$ (3 points) in the results are shown in figure 8:

- Chebyshev-Gauss-Lobatto (CGL): 0.0000, 0.5000, 1.0000.
- Legendre-Gauss-Lobatto (LGL): 0.0000 0.6667 1.0000.
- Uniform: 0.0000, 0.5000, 1.0000.

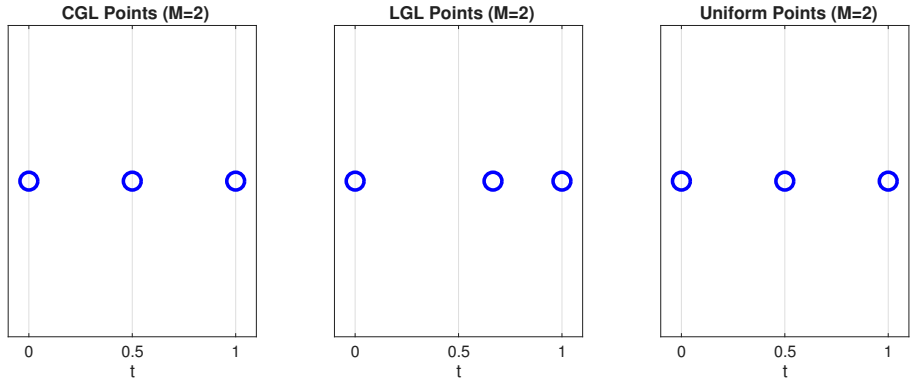

Figure 8: Three types of collocation points were tested with $\nu = 2$ (3 points).

Table 5 presents the numerical results obtained with each collocation point type.

Table 5: Numerical results for example 3 with $\xi = 0.5$, $\nu = 2$.

Points	J	$\max \lvert X - X_{\text{exact}} \rvert$	$\max \lvert V - V_{\text{exact}} \rvert$
CGL	5.78×10^{-32}	4.44×10^{-16}	4.44×10^{-16}
LGL	1.51×10^{-31}	6.66×10^{-16}	6.66×10^{-16}
Uniform	5.71×10^{-32}	4.44×10^{-16}	4.44×10^{-16}

The exact solution recovery is illustrated in figure 9. In the figures 10, 11, 12 and 13, we present a comparison of absolute errors for example 3 showing exact recovery for $\xi = 0.5$ and different ν.

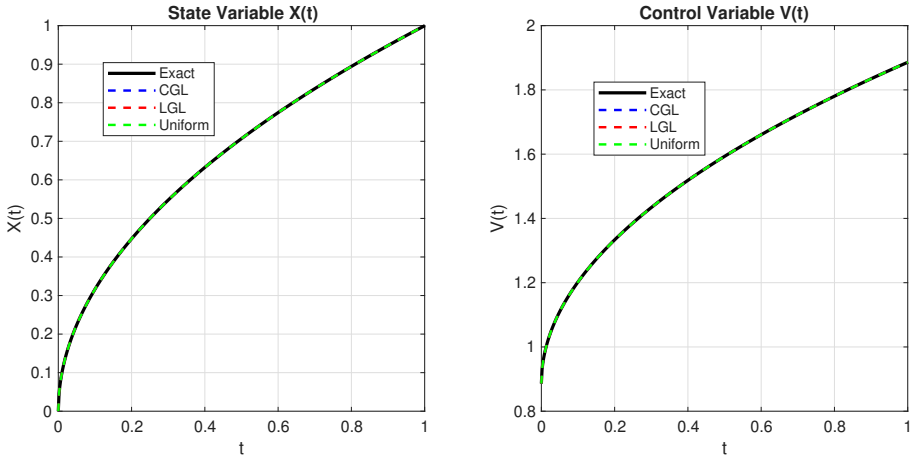

Figure 9: Comparison of approximate and exact solutions for example 3 showing exact recovery for $\xi = 0.5$ and $\nu = 2$.

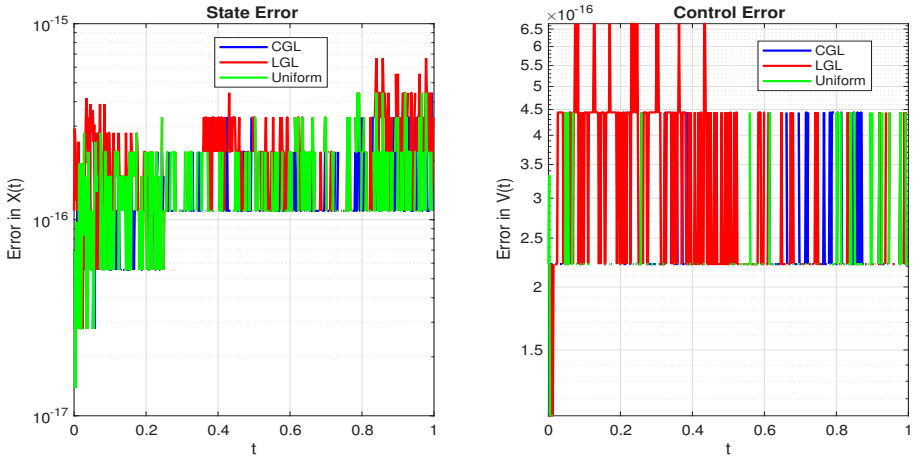

Figure 10: Comparison of absolute errors for example 3 showing exact recovery for $\xi = 0.5$ and $\nu = 2$.

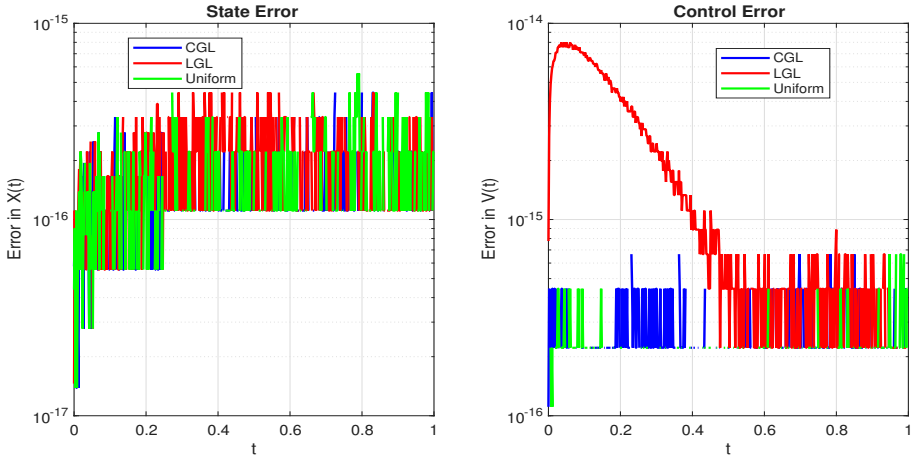

Figure 11: Comparison of absolute errors for example 3 showing exact recovery for $\xi = 0.5$ and $\nu = 4$.

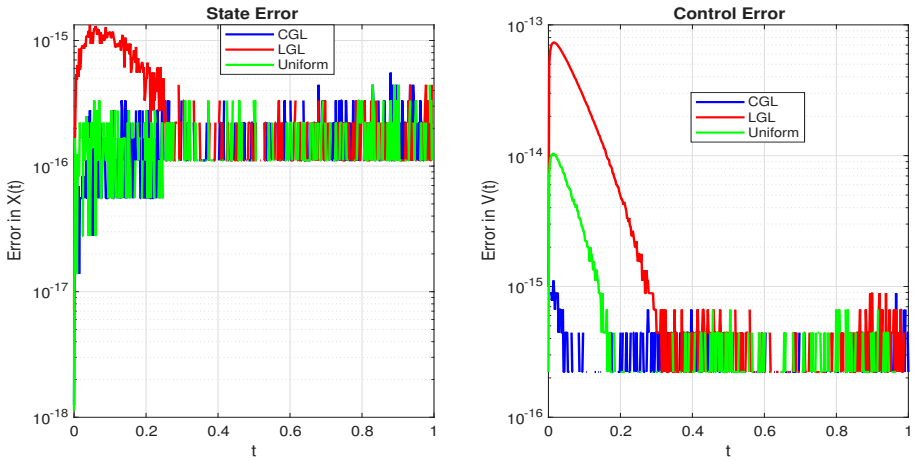

Figure 12: Comparison of absolute errors for example 3 showing exact recovery for $\xi = 0.5$ and $\nu = 6$.

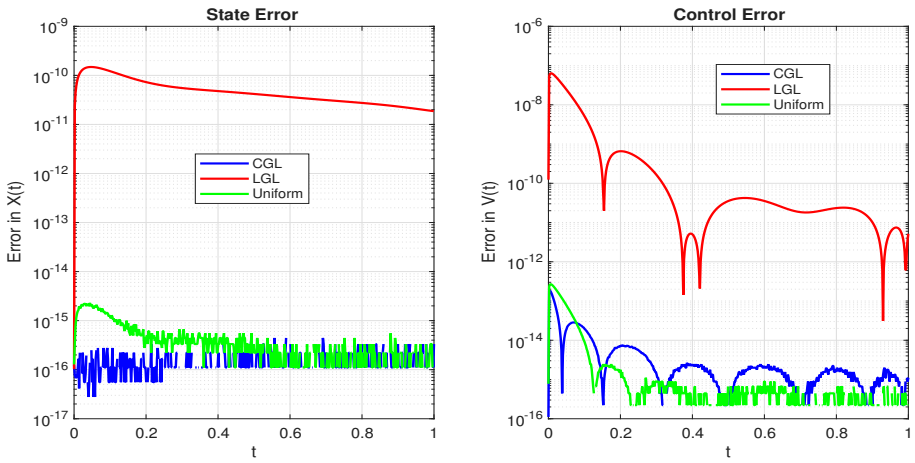

Figure 13: Comparison of absolute errors for example 3 showing exact recovery for $\xi = 0.5$ and $\nu = 8$.

Table 6 presents the CPU time comparison for different ν values for example 3. The computational complexity of the proposed method is $\mathcal{O}(\nu^3)$ due to matrix inversion ($\mathbf{S}^{-1}$) and Newton iterations, while memory complexity is $\mathcal{O}(\nu^2)$. For $\nu \leq 8$, the method runs in under 0.08 seconds on a standard desktop computer.

Table 6: CPU time comparison for different ν values (example 3).

ν	**CGL (s)**	**LGL (s)**	**Uniform (s)**
2	0.0207	0.0038	0.0039
4	0.0155	0.0152	0.0100
8	0.0521	0.0603	0.0762

Conclusion

A collocation scheme for MFOPCs based on expansion via Mittag-Leffler functions was proposed in the present work. Main contributions from the present study comprise the following: (i) the creation of an innovative operational matrix for fractional differentiation; (ii) systematic handling of inequality constraints by means of the slack variable approach integrated with the Mittag-Leffler framework; (iii) rigorous proof of convergence of the proposed scheme for analytic functions; (iv) numerical implementation on three examples with comparison of CGL, LGL, and uniform collocation nodes; and (v) demonstration that the method exactly recovers fractional-power solutions when they lie in the approximation space. Further research should examine the applications of the proposed scheme to distributed-order FOPCs, FOPCs subject to state constraints, MFOCPs in higher dimensions based on tensor product expansions, and adaptive approaches for singular solutions of FOPCs.

Conflicts of interests

There is no conflict of interest in this work.

Acknowledgments

The author would like to thank the referees for their useful comments and remarks.

Availability of data and materials

Not applicable.

Competing interests

The authors declare that they have no competing interests.

Data availability

Not applicable.

References

[1] M.H. Heydari, M.R. Hooshmandasl, F.M.M. Ghaini, and C. Cattani. Wavelets method for solving fractional optimal control problems. *Applied Mathematics and Computation*, 286:139–154, 2016.

[2] I. Podlubny. *Fractional differential equations: an introduction to fractional derivatives, fractional differential equations, to methods of their solution and some of their applications*, volume 198. Elsevier, 1998.

[3] L. Sadek and A. Algefary. The cotangent derivative with respect to another function: Theory, methods and applications. *Fractal and Fractional*, 9(11):690, 2025.

[4] M. Alqhtani, L. Sadek, and K.M. Saad. The mittag-leffler–caputo–fabrizio fractional derivative and its numerical approach. *Symmetry*, 17(5):800, 2025.

[5] L. Sadek, S. Ounamane, B. Abouzaid, and E.M. Sadek. The galerkin bell method to solve the fractional optimal control problems with inequality constraints. *Journal of Computational Science*, 77:102244, 2024.

[6] S. Ounamane, L. Sadek, B. Abouzaid, and E.M. Sadek. Fractional truncated exponential method for linear fractional optimal control problems. *Mathematics and Computers in Simulation*, 232:408–426, 2025.

[7] S. Ounamane, L. Sadek, B. Abouzaid, and E.M. Sadek. Fractional truncated exponential technique to solve the optimal control atangana–baleanu problems. *The Journal of Supercomputing*, 82(3):113, 2026.

[8] O. Abu Arqub and N. Shawagfeh. Solving optimal control problems of fredholm constraint optimality via the reproducing kernel hilbert space method with error estimates and convergence analysis. *Mathematical Methods in the Applied Sciences*, 44(10):7915–7932, 2021.

[9] H. Badawi, O.A. Arqub, and N. Shawagfeh. Well-posedness and numerical simulations employing legendre-shifted spectral approach for caputo–fabrizio fractional stochastic integrodifferential equations. *International Journal of Modern Physics C*, 34(6):2350070, 2023.

[10] H. Badawi, O.A. Arqub, and N. Shawagfeh. Existence, uniqueness, and collocation solutions using the shifted legendre spectral method for the hilfer fractional stochastic integro-differential equations regarding stochastic brownian motion. *Results in Applied Mathematics*, 24:100504, 2024.

[11] H. Badawi, O.A. Arqub, and N. Shawagfeh. Theoretical study and numerical analysis using step spectral collocation method for stochastic m-fractional differential models of simplified brownian motion within constant delays process. *Journal of Applied Mathematics and Computing*, 71(5):6773–6805, 2025.

[12] B. Kafash, A. Delavarkhalafi, and S.M. Karbassi. Application of chebyshev polynomials to derive efficient algorithms for the solution of optimal control problems. *Scientia Iranica*, 19(3):795–805, 2012.

[13] H.R. Marzban and S.S. Korooyeh. Optimal control of linear fractional-order delay systems with a piecewise constant order based on a generalized fractional chebyshev basis. *Journal of Vibration and Control*, 29(17-18):4257–4274, 2023.

[14] M.H. Heydari, M. Razzaghi, and Z. Avazzadeh. Orthonormal piecewise bernoulli functions: Application for optimal control problems generated using fractional integro-differential equations. *Journal of Vibration and Control*, 29(5–6):1164–1175, 2023.

[15] S. Hosseinpour and A. Nazemi. A collocation method via block-pulse functions for solving delay fractional optimal control problems. *IMA Journal of Mathematical Control and Information*, 34(4):1215–1237, 2017.

[16] Y. Gu, H. Yan, and Y. Zhu. A numerical method for solving optimal control problems via legendre polynomials. *Engineering Computations*, 37(8):2735–2759, 2020.

[17] S.A. Yousefi, A. Lotfi, and M. Dehghan. The use of a legendre multiwavelet collocation method for solving the fractional optimal control problems. *Journal of Vibration and Control*, 17(13):2059–2065, 2011.

[18] K. Maleknejad and A. Ebrahimzadeh. The use of rationalized haar wavelet collocation method for solving optimal control of volterra integral equations. *Journal of Vibration and Control*, 21(10):1958–1967, 2015.

[19] I. Pakravan, A. Heidari Soureshjani, R. Talebitooti, and M. Talebitooti. Haar wavelet technique applied on the functionally graded carbon nanotube reinforced conical shells to study free vibration and buckling behaviors in thermal environments. *Journal of Vibration and Control*, 28(15-16):1863–1878, 2022.

[20] A. Yari and M.K. Mirnia. Solving optimal control problems by using hermite polynomials. *Computational Methods for Differential Equations*, 8(2):314–329, 2020.

[21] S. Sabermahani and Y. Ordokhani. Fibonacci wavelets and galerkin method to in-

vestigate fractional optimal control problems with bibliometric analysis. *Journal of Vibration and Control*, 27(15-16):1778–1792, 2021.

[22] N. Kumar and M. Mehra. Generalized fractional-order legendre wavelet method for two dimensional distributed order fractional optimal control problem. *Journal of Vibration and Control*, 30(7-8):1690–1705, 2024.

[23] N. Kumar and M. Mehra. Legendre wavelet collocation method for fractional optimal control problems with fractional bolza cost. *Numerical Methods for Partial Differential Equations*, 37(2):1693–1724, 2021.

[24] A.A. Kilbas, Hari M. Srivastava, and J.J. Trujillo. *Theory and applications of fractional differential equations*, volume 204 of *North-Holland Mathematics Studies*. 2006.

[25] M. Alipour, D. Rostamy, and D. Baleanu. Solving multi-dimensional fractional optimal control problems with inequality constraint by bernstein polynomials operational matrices. *Journal of Vibration and Control*, 19(16):2523–2540, 2013.

[26] L.N. Trefethen. *Approximation theory and approximation practice, extended edition*. Society for Industrial and Applied Mathematics, 2019. https://lccn.loc.gov/2019027108.